J Mater Sci (2010) 45:3824–3832
DOI 10.1007/s10853-010-4437-0

# Effect of pH value on the synthesis and characterization of $Ba_{0.5}Sr_{0.5}Co_{0.8}Fe_{0.2}O_{3-\delta}$ powders prepared by the citrate–EDTA complexing method

**I.-Ming Hung · Chen-Yu Liang · Chun-Jing Ciou · Ren-Zheng Song · Zu-Yu Lai**

Received: 21 October 2009 / Accepted: 23 March 2010 / Published online: 2 April 2010


**Abstract** This study reports the successful preparation of potential candidate $Ba_{0.5}Sr_{0.5}Co_{0.8}Fe_{0.2}O_{3-\delta}$ (BSCF) oxides for intermediate-temperature solid oxide fuel cells (IT-SOFCs) by a combined citrate-ethylenediaminetetraacetic acid (EDTA) complexing method. The resulting crystal properties, chemical composition, conductivity, and electrochemical properties were studied by X-ray diffraction (XRD), inductively coupled plasma mass spectroscopy (ICP-MS), energy dispersive spectrum (EDS), four-point DC measurement and AC impedance. The X-ray diffraction results of all samples with different pH values reveal a basic perovskite structure. Although samples prepared from different pH solutions have a similar structure, their chemical composition and grain morphologies are different. The optimized composition of BSCF is the sample prepared from the precursor solution with a pH value of 6; this produced highest conductivity at 50.2 S/cm at 400 °C, which is 1.3 times higher than the sample prepared from the precursor solution with a pH value of 9. Electrochemical impedance spectra at an intermediate temperature reveal the better electrochemical performance of BSCF electrode prepared from the solution with pH of 6. The lowest polarization resistance values for charge transfer and oxygen diffusion are 0.07 and 0.11 Ω $cm^2$ at 800 °C, respectively.

I.-M. Hung (✉) · C.-Y. Liang · C.-J. Ciou · R.-Z. Song · Z.-Y. Lai
Yuan Ze Fuel Cell Center/Department of Chemical Engineering and Materials Science, Yuan Ze University, No. 135, Yuan-Tung Road, Chungli, Taoyuan 320, Taiwan
e-mail: imhung@saturn.yzu.edu.tw

## Introduction

Solid oxide fuel cells (SOFCs) directly convert chemical energy into heat and electricity without involving combustion cycles. Comparing with traditional energy technology, SOFCs have many advantages, such as high-energy conversion efficiency, high power density, low pollution, and flexibility in using hydrocarbon fuels [1]. Conventional SOFCs operate at high temperatures of around 800–1000 °C. However, this high temperature leads to many disadvantages, including unwanted chemical reactions between components, a long warm-up period, and the requirement of using an expensive ceramic conductor as an interconnector, etc. If the operation temperature of SOFCs could be decreased to 600–800 °C, inexpensive stainless steel could be used as the interconnector; and the chemical and thermal durability of all the components would be increased. However, the conductivity of the cathode material would also decrease, and the activation polarization of the cathode electrode would increase significantly at lower temperatures. Therefore, the development of high performance cathode materials is an important issue for intermediate-temperature SOFCs (IT-SOFCs).

Among various perovskite cathodes, the (La, Sr)(Co, Fe)$O_{3-\delta}$ (LSCF) oxides have been widely investigated as cathodes for IT-SOFCs working below 800 °C. The high catalytic activity of LSCF is due to rapid surface exchange kinetics and high oxygen vacancy concentration [2]. In 1985, Teraoka et al. reported a $SrCo_{0.8}Fe_{0.2}O_{3-\delta}$ (SCF) membrane with a very high oxygen permeation flux due to a high concentration of oxygen vacancies [3]. In 2001, Huang et al. used SCF as a cathode material for SOFCs, but the SCF is not stable at lower oxygen partial pressures [4]. In 2000, Shao et al. [5] widely investigated $Ba_{0.5}Sr_{0.5}Co_{0.8}Fe_{0.2}O_{3-\delta}$

(BSCF) as an oxygen separation membrane, and found that the BSCF exhibits high oxygen permeation and acceptable conductivity. Recently, researchers used BSCF as a new cathode material for IT-SOFCs [6]. This IT-SOFC exhibits a high power density of 1010 mW/cm$^2$ at 600 °C when using hydrogen as the fuel and air as the cathode gas.

Researchers generally agree that the oxygen electroreduction process in a cathode electrode is a multistep electrochemical process, including (1) diffusion of $O_2$ from the gas phase to the surface of cathode; (2) dissociation of the chemisorbed oxygen molecule into atomic oxygen at the active site; (3) charge transfer; (4) diffusion of $O^{2-}$ from the cathode electrode to the cathode/electrolyte interface and into the electrolyte [7]. The excellent electrochemical performance of BSCF can be attributed to its high oxygen vacancy and high rate of oxygen diffusion. In fact, the oxygen diffusion flux of cathode electrode is affected both in the chemical composition and the microstructure. Previous study shows that oxygen diffusion flux increases as the average grain size of BSCF materials decreases [8]. However, the desired stoichiometric composition is the major factor for determining the oxygen diffusion flux rate of BSCF prepared from different synthesis methods.

Recently, BSCF has been widely prepared by the citrate-ethylenediaminetetraacetic acid (EDTA) complexing method and several studies have investigated the electrochemical characterization of the sample [9–11]. Lee et al. reported that a BSCF electrode prepared from a precursor solution with a pH value of 8 showed the best electrochemical performance [12]. However, there are few published results about the characterization of BSCF oxides prepared by citric–edta from precursor solutions with different pH values. Therefore, this study reports the synthesis of BSCF by the citric–edta complexing method with different pH precursor solutions. This study also investigates the characterization, conductivity, and the electrochemical performance of all samples.

## Experimental

BSCF powders were prepared using the citrate–edta complexing method. First, 0.04 mol of ethylenediaminetetraacetic acid (EDTA, Riedel–dehaen, 98%) was mixed with 50 mL of 13 N $NH_4OH$ solution to make a $NH_3$-EDTA solution. Then, 0.01 mol of $Ba(NO_3)_2$ (J. T. Baker, 99.6%) was added to the $NH_3$-EDTA solution, which was then heated and stirred. Next, 0.01 mol of $Sr(NO_3)_2$ (Alfa Aesar, 99.0%), 0.016 mol of $Co(NO_3)_2{\cdot}6H_2O$ (J. T. Baker, 99.8%), and 0.004 mol of $Fe(NO_3)_3{\cdot}9H_2O$ (Alfa Aesar, 98.0–101.0%) were dissolved in the other $NH_3$-EDTA solution. These two solutions were mixed and stirred, then 0.06 mol of citric acid was added to the mixed solution. The mole ratios of EDTA:citric acid:total metal ions were 1:1.5:1. The pH value was adjusted to 5, 6, 8, 9, and 10 in different solution samples by adding different amounts of $NH_4OH$ solution (designed as pH5-BSCF, pH6-BSCF, pH8-BSCF, pH9-BSCF, and pH10-BSCF). Each solution was heated on a hotplate at 100 °C and stirred until the water evaporated and a sticky gel formed. The gelled BSCF precursors were then heated at 200 °C for 3 h. After heat treatment, the samples were calcined at 950 °C for 12 h. Finally, the samples were sintered at 1050 °C for 5 h.

The phase identification of the BSCF powders was performed with a powder diffractometer (LabX, XRD-6000) with Ni-filtered Cu Kα radiation, and a diffraction angle from 20° to 80° with a step of 0.01° and a rate of 1°/min. The weight loss of BSCF6 sample as function as temperature was measured by thermogravimetric analysis (TGA, PerkinElmer Pyris 1) with heating rate of 5 °C/min in air. The chemical composition of all samples was analyzed by inductively coupled plasma mass spectroscopy (ICP-MS, Perkin Elmer, SCIEX ELAN 5000) and energy dispersive spectrum (EDS). The EDS analysis measured at least 10 points. The conductivity was measured in air by the DC four-terminal method using Agilent Technologies 34970A and 6645A data acquisition/switch units with silver as the metallic electrode and wire from room temperature to 800 °C. The BSCF rods were dry pressed on 25 MPa and sintered at 1050 °C for 5 h. The rod size is about 10 mm long, 2 mm wide, and 2 mm thick. The morphologies of the sintered BSCF electrode were observed by field emission scanning electron microscopy (FE-SEM, Jeol 6701F). The average grain size was calculated by the linear intercept method using the relation $G = 1.5L/MN$ where 1.5 is a geometry dependent proportionality constant, $L$ is the total test line length, $M$ is the magnification, and $N$ is the total number of intercepts. The electrochemical impedance spectra (EIS) of the BSCF-30 wt% $Ce_{0.8}Sm_{0.2}O_{1.9}$ (BCSF-SDC) composite cathode were measured by using a three-electrode cell. BSCF-30 wt% $Ce_{0.8}Sm_{0.2}O_{1.9}$ (SDC, Gimat) composite films were screen printed on one side of SDC disks to prepare cells for electrochemical impedance spectroscopy (EIS). The SDC substrate disks, 10 mm in diameter and 0.5 mm thick, were prepared by solid-state method and sintering at 1550 °C for 6 h. A slurry with proper viscosity for screen printing was typically obtained by ball-milling a mixture of 0.3 g BSCF powder with 0.13 g SDC powder and 0.0258 g ethyl cellulose-terpineol (J. T. Baker) binder. After screen printing, the cells were baked at 120 °C and then sintered at 1050 °C for 5 h. Pt was used as the reference and counting electrodes on the other side of the electrolyte. The EIS was measured using an impedance analyzer (HIOKI,

3532-50) set to 30 mV over a frequency range from 1000 kHz to 0.01 Hz.

## Results and discussion

To confirm the formation of the BSCF oxide, the samples were analyzed using XRD. Figure 1 presents the XRD patterns of the BSCF powders. The five kinds of BSCF powders, which were prepared from precursor solutions with different pH solutions, were well indexed as a single-phase cubic $ABO_3$ perovskite-type structure with a lattice parameter ranging from 3.985 to 3.987 Å. This result shows that the samples prepared from the precursor solutions with different pH values exhibited the same structure and phases. Figure 2 shows the morphologies of the BSCF electrodes prepared from precursor solutions with different pH values and sintered at 1050 °C for 5 h. The grain size and porosity of all samples were shown in Table 1. The porosity of samples was between 13.7 and 17.7%, as measured by the Archimedes method. The grain size of BSCF electrodes increased from 6.9 to 9.3 μm as the pH value of precursor increased from 5 to 10.

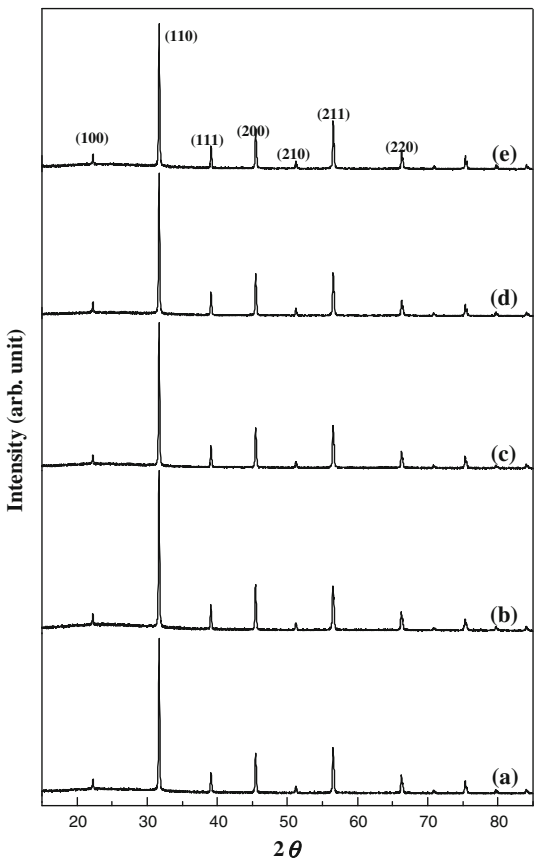


**Fig. 1** XRD patterns of (*a*) pH5-BSCF, (*b*) pH6-BSCF, (*c*) pH8-BSCF, (*d*) pH9-BSCF, and (*e*) pH10-BSCF electrodes

A high electronic conductivity is important because it may produce a good current-collecting efficiency and a low ohmic resistance for an IT-SOFC cathode. Due to the co-existence of electron holes and oxygen vacancies, there are electronic and ionic conductivity mechanisms in a mixed ionic and electronic conductor (MIEC). However, the ionic conductivity is much lower than the electric conductivity. Therefore, the conductivity measured by the DC 4 terminal method in this study can be believed to occur by the hopping of p-type plarons and associated with the behaviors of the multivalent state Co and Fe cations [13, 14]. Sintering conditions also influence the performance of a BSCF electrode. The bonding between BSCF and the $Ce_{0.8}Sm_{0.2}O_{1.9}$ (SDC) electrolyte is poor if the sintering temperature is as low as 900 °C. However, a chemical reaction will occur between BSCF and SDC at temperatures above 1100 °C. Therefore, the BSCF electrodes sintered at 1050 °C on the SDC electrolyte have the best performance. Figure 3 shows the temperature dependence of the total electrical conductivity of all BSCF samples sintered at 1050 °C for 5 h in air. This figure shows that the electrical conductivity of all the samples prepared from precursors with different pH values first increases gradually with temperature, reaches a maximum value at 400 °C, and then decreases as the operation temperature continues to rise. The sample prepared from the precursor solution with a pH of 6 exhibited the highest conductivity at 50.2 S/cm, which is about 33% higher than that of the sample prepared from the precursor solution with a pH of 9 (37.7 S/cm). The conductivity of all samples decreases as the temperature exceeds 400 °C. The temperature at which the samples exhibit maximum conductivity in this study is much higher than the reported of conductivity of about 33 S/cm at 570 °C by Wei et al. [10], but similar to that reported by Shao and coworkers [15]. This difference may be due to slight variation in chemical composition. Although the conductivity of all samples is lower than that of cathode materials, such as $La_{0.8}Sr_{0.2}Co_{0.8}Fe_{0.2}O_{3-\delta}$ (LSCF) [16], the loss of lattice oxygen upon heating can lead to the formation of oxygen vacancies in BSCF. Therefore, BSCF should exhibit higher oxygen ionic conductivity than LSCF, not only on the triple-phase boundary but also on the surface of the electrode. This is an important reason why BSCF exhibits better electrochemical performance [17].

If the carrier concentration remains constant throughout the temperature range measurement, the Arrhenius plots of polaron conduction should be linear, following the formula relation:

$$\sigma = A/T\exp(-E_a/kT) \quad (1)$$

Fig. 4 and Table 2 provide the Arrhenius plot and calculated activation energies $E_a$ using the linear part in the two

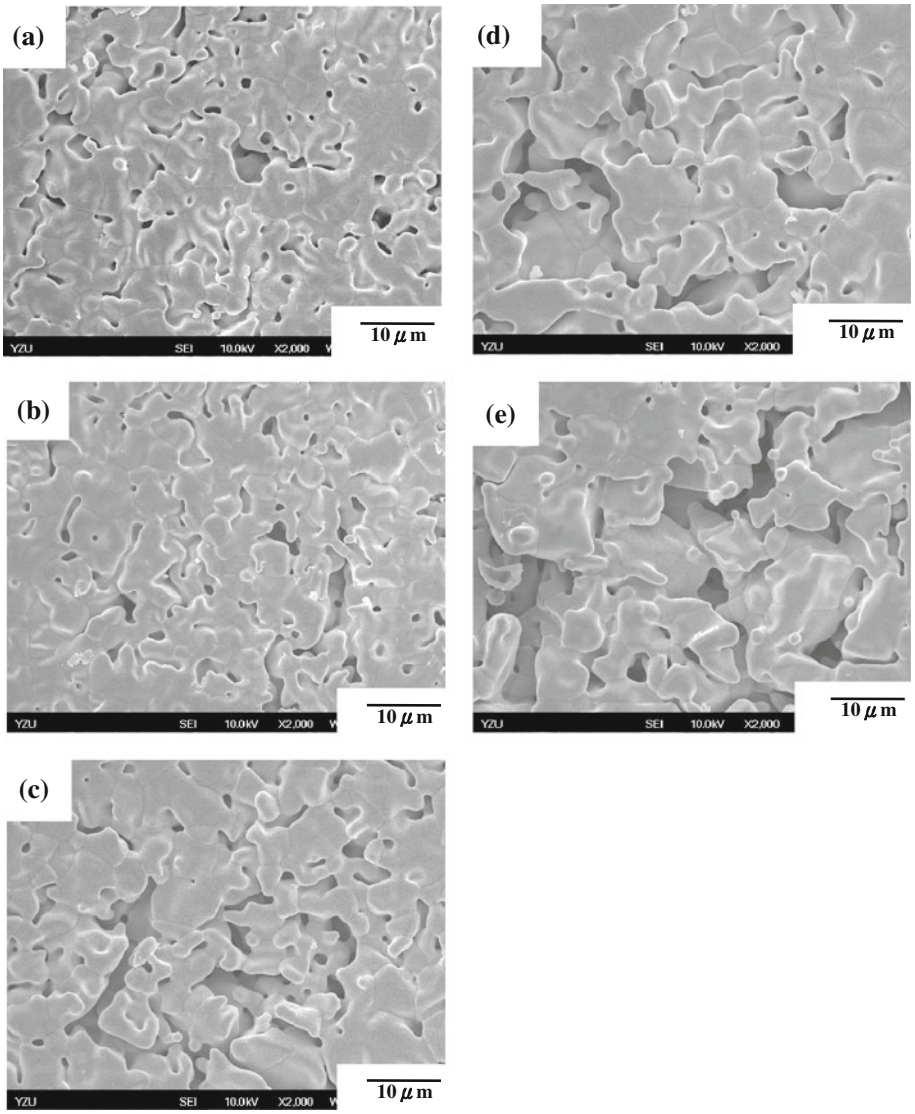


**Fig. 2** SEM pictures of **a** pH5-BSCF, **b** pH6-BSCF, **c** pH8-BSCF, **d** pH9-BSCF, and **e** pH10-BSCF electrodes sintered at 1050 °C for 5 h

**Table 1** The average grain size and porosity of BSCF electrodes prepared from precursor solutions with different pH values

| Samples | Average grain size (μm) | Porosity (%) |
|---|---|---|
| pH5-BSCF | 6.9 ± 0.74 | 15.1 |
| pH6-BSCF | 7.0 ± 1.16 | 13.7 |
| pH8-BSCF | 7.9 ± 1.56 | 16.4 |
| pH9-BSCF | 8.8 ± 1.95 | 14.6 |
| pH10-BSCF | 9.3 ± 1.68 | 17.7 |

temperature ranges 50–400 and 400–750 °C for all samples. The activation energy ($E_{a1}$) ranges from 24 to 25 kJ/mole for all samples at temperatures between 50 and 450 °C, which is much lower than the data reported by Wei et al. [10] but similar to the data reported by Wang et al. [18]. The activation energy ($E_{a2}$) of all samples ranges from 2.0 to 4.6 kJ/mole in the temperature range 400–750 °C. Note that the value of $E_{a2}$ is much lower than that

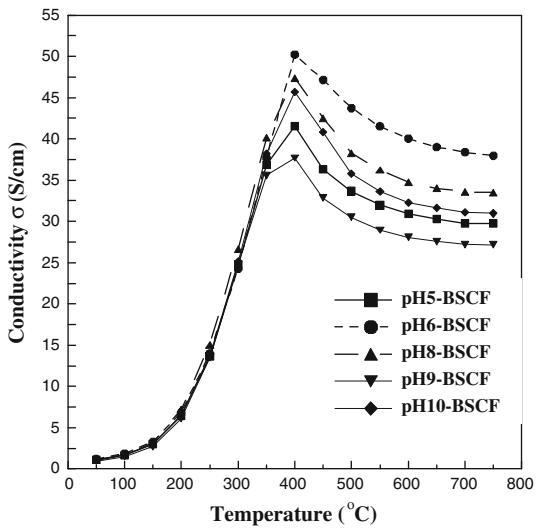


**Fig. 3** Conductivity of pH5-BSCF, pH6-BSCF, pH8-BSCF, pH9-BSCF, and pH10-BSCF electrodes at various temperatures

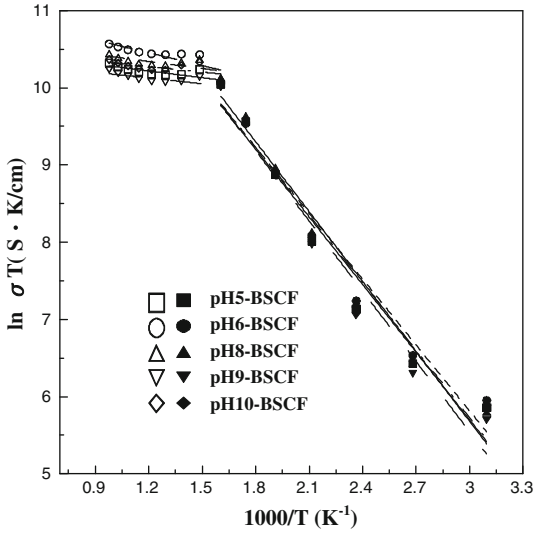


**Fig. 4** Arrhenius plot of the conductivity of pH5-BSCF, pH6-BSCF, pH8-BSCF, pH9-BSCF, and pH10-BSCF electrodes

**Table 2** Activation energy of BSCF electrodes prepared from precursor solutions with different pH values

| Samples | $E_{a1}$ (KJ/mole, 50–400 °C) | $E_{a2}$ (KJ/mole, 400–750 °C) |
|---|---|---|
| pH5-BSCF | 24 | 2.4 |
| pH6-BSCF | 24 | 4.6 |
| pH8-BSCF | 25 | 2.5 |
| pH9-BSCF | 25 | 2.0 |
| pH10-BSCF | 24 | 2.0 |

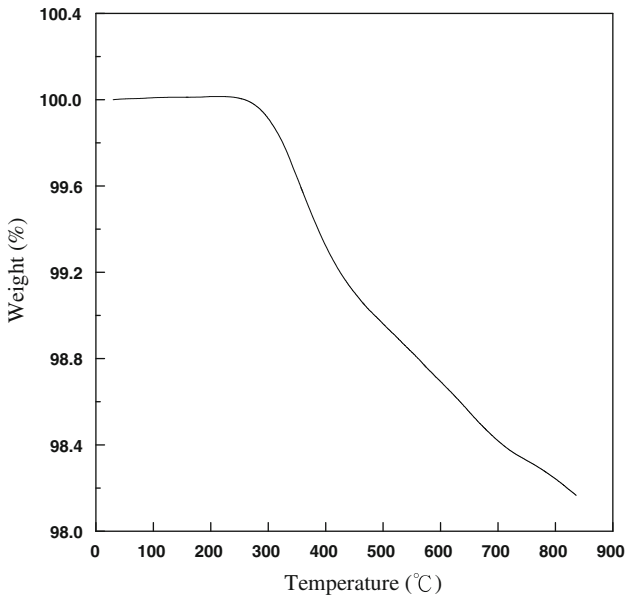


**Fig. 5** TGA curve of pH6-BSCF with heating rate of 5 °C/min in air

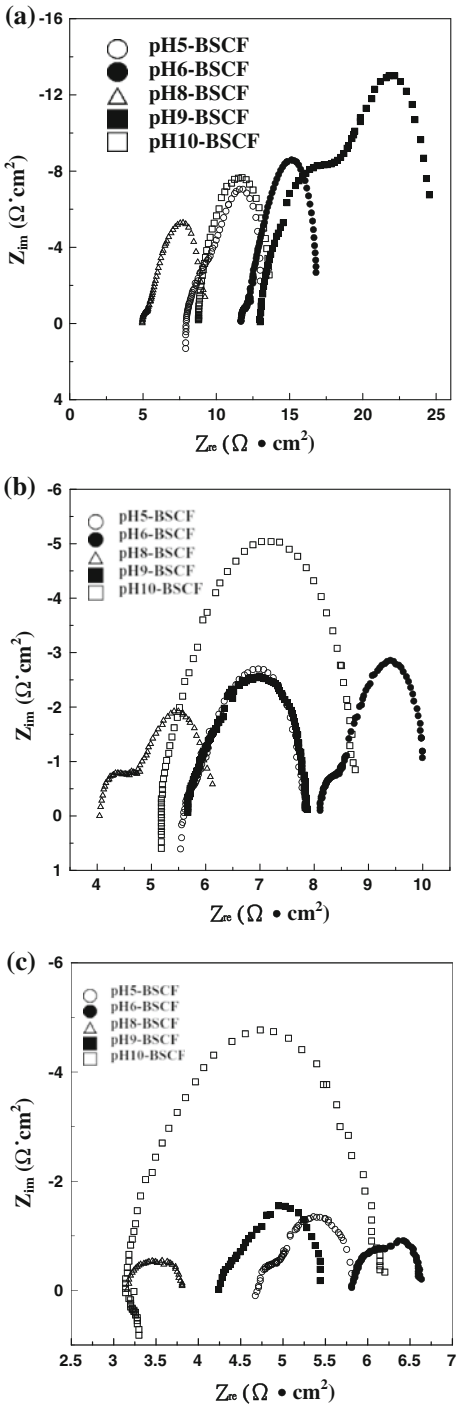


**Fig. 6** Impedance spectra of Pt/SDC/BSCF cells. The operating temperature was **a** 600 °C, **b** 650 °C, and **c** 700 °C

of $E_{a1}$, only 10% of $E_{a1}$. The approximate $E_a$ of these samples means that samples prepared from precursor solutions with different pH values share a similar conduction mechanism. Figure 5 shows the thermogravimetric analysis (TGA) of the BSCF6 sample in air. There is an apparently weight loss of BSCF as temperature above

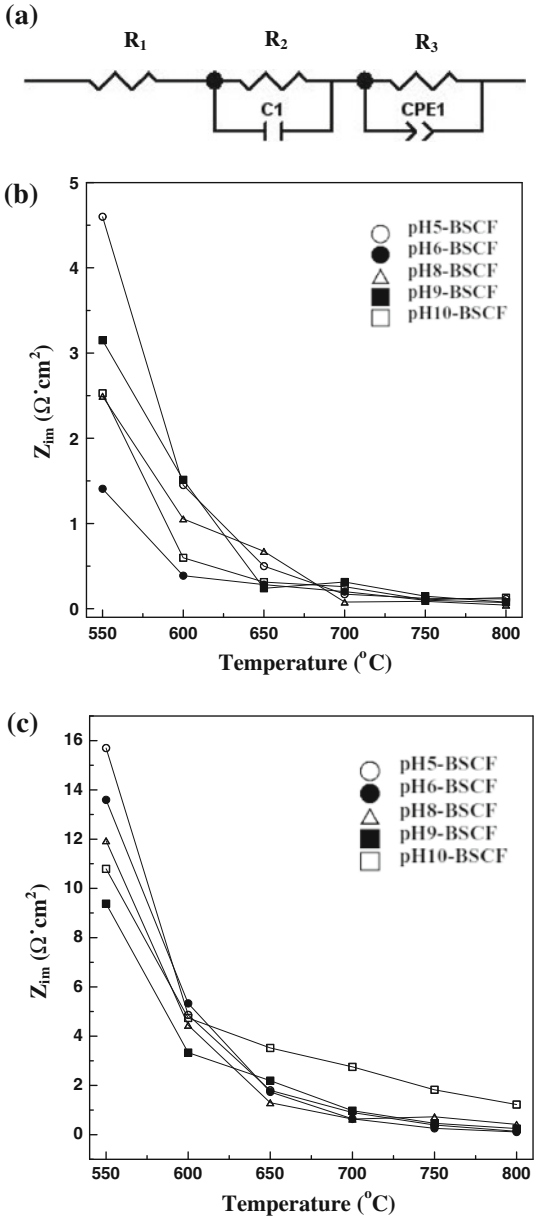


**Fig. 7** **a** equivalent circuit for AC impedance spectra and **b** $R_2$ resistance and **c** $R_3$ resistance of BSCF electrodes as a function of temperature

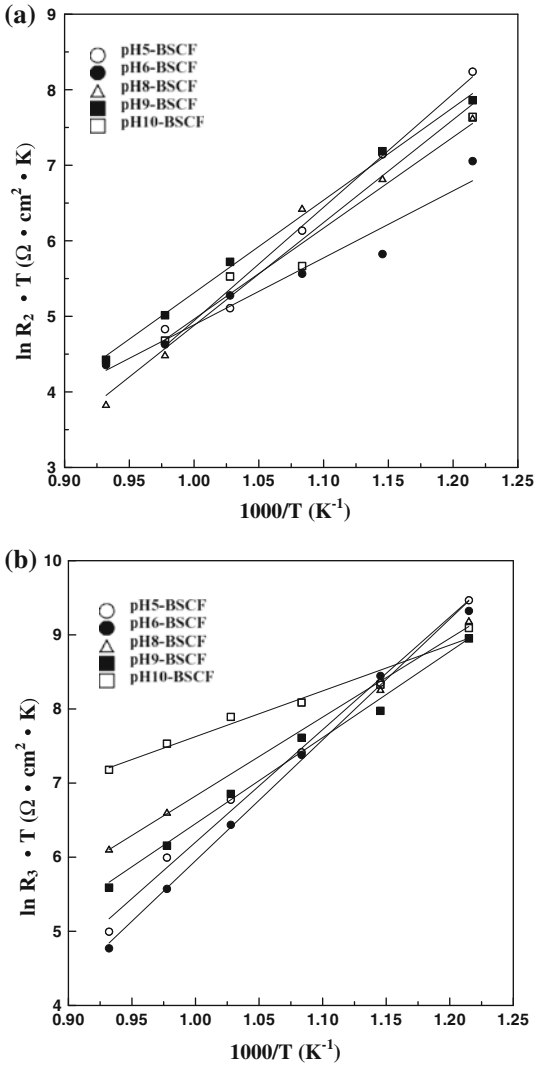


**Fig. 8** Arrhenius plots of **a** $R_2$ resistance and **b** $R_3$ resistance of BSCF electrodes prepared from various pH values

400 °C that is due to the loss of oxygen and formation of oxygen vacancies in BSCF.

The concentration of charged carries of BSCF depends on the oxygen partial pressure, ratio of A-site and B-site

**Table 3** Impedance spectra fitting results at different temperatures

| Temperature (°C) | pH5-BSCF | | pH6-BSCF | | pH8-BSCF | | pH9-BSCF | | pH10-BSCF | |
|---|---|---|---|---|---|---|---|---|---|---|
| | $R_2$ (Ω cm$^2$) | $R_3$ (Ω cm$^2$) | $R_2$ (Ω cm$^2$) | $R_3$ (Ω cm$^2$) | $R_2$ (Ω cm$^2$) | $R_3$ (Ω cm$^2$) | $R_2$ (Ω cm$^2$) | $R_3$ (Ω cm$^2$) | $R_2$ (Ω cm$^2$) | $R_3$ (Ω cm$^2$) |
| 550 | 4.60 | 15.7 | 1.41 | 13.6 | 2.49 | 11.9 | 3.15 | 9.38 | 2.53 | 10.8 |
| 600 | 1.45 | 4.86 | 0.39 | 5.33 | 1.05 | 4.45 | 1.51 | 3.33 | 0.60 | 4.74 |
| 650 | 0.50 | 1.80 | 0.28 | 1.74 | 0.67 | 1.30 | 0.24 | 2.19 | 0.31 | 3.52 |
| 700 | 0.17 | 0.90 | 0.20 | 0.64 | 0.08 | 0.63 | 0.31 | 0.97 | 0.26 | 2.75 |
| 750 | 0.12 | 0.39 | 0.10 | 0.26 | 0.09 | 0.72 | 0.15 | 0.46 | 0.11 | 1.82 |
| 800 | 0.11 | 0.14 | 0.07 | 0.11 | 0.04 | 0.42 | 0.08 | 0.25 | 0.13 | 1.22 |

**Table 4** Activation energy of BSCF electrodes prepared from precursor solutions with different pH values

| Samples | $E_{aR_2}$ (KJ/mole) | $E_{aR_3}$ (KJ/mole) |
|---|---|---|
| pH5-BSCF | 125 | 126 |
| pH6-BSCF | 74 | 136 |
| pH8-BSCF | 113 | 88 |
| pH9-BSCF | 102 | 97 |
| pH10-BSCF | 100 | 51 |

cations, and valences of B-site cations. Under $P_{O_2} = 0.21$ atm, the filling of oxygen vacancies will produce electron holes according to Eq. 2 as followed:

$$\frac{1}{2}O_{2(g)} + V_O^{\bullet\bullet} \rightarrow O_O^{\times} + 2h^{\bullet} \quad (2)$$

From the results of conductivity and TGA data, it can be inferred that the BSCF samples were the p-type conductor below 673 K in air. The conductivity of this p-type BSCF conductor increases hopping between $Co^{3+}$ and $Co^{4+}$ or $Fe^{3+}$ and $Fe^{4+}$. At the temperature above 400 °C, electrons are produced due to the formation of oxygen vacancies, according to Eq. 3 as follows:

$$O_O^{\times} \rightarrow 2e' + V_O^{\bullet\bullet} + \frac{1}{2}O_2 \quad (3)$$

The conductivity contributed from electron holes decreases as the electron concentration increases due to formation of oxygen vacancies at temperature above 400 °C. Along with the formation of oxygen deficiency, it causes the thermal reduction of Co and Fe cations to lower states. To retain electrical neutrality, the reduction of the Fe and Co ions, which is expected to occur, can be described in Eqs. 4 and 5, respectively:

$$2Co_{Co}^{\bullet} + O_O^{\times} \leftrightarrow 2Co_{Co}^{\times} + V_O^{\bullet\bullet} + \frac{1}{2}O_2 \quad (4)$$

$$2Fe_{Fe}^{\bullet} + O_O^{\times} \leftrightarrow 2Fe_{Fe}^{\times} + V_O^{\bullet\bullet} + \frac{1}{2}O_2 \quad (5)$$

This phenomenon arises from hopping between $Co^{3+}/Co^{2+}$ and $Fe^{3+}/Fe^{2+}$. Therefore, the decrease in concentration of electron holes results in low activation energy ($E_{a2}$) from the ln $\sigma T$ versus $1/T$ graphs.

Figure 6a–c show the impedance spectra of BSCF electrodes prepared from different pH value solutions on SDC electrolyte measured at 600, 650, and 700 °C in air. Figure 7a presents the equivalent circuit. The elements of the equivalent circuit correspond to the electrochemical process: $R_1$ corresponds to the resistance of electrolyte, $R_2$ corresponds to the resistance of charge transfer process, and the $R_3$ corresponds to the diffusion resistance of oxygen [19–21]. Figure 7b and c and Table 3 show the fitting results of $R_2$ and $R_3$. The charge transfer resistances of BSCF electrodes prepared from the precursor solution with a pH value of 6 are lower than that of other BSCF electrodes at all operating temperatures, especially in the low temperature range from 550 to 650 °C. However, the pH9-BSCF electrode prepared from the precursor solution with a pH of 9 showed a lower oxygen diffusion resistance than other samples in the temperature range from 550 to 650 °C. The pH6-BSCF electrode showed the lowest area specific resistance (ASR) of $R_2$ and $R_3$ resistances of 0.07 and

**Table 5** ICP-MS and EDS analysis of BSCF powders prepared from precursor solutions with different pH values

| | ICP-MS | | | | | | |
|---|---|---|---|---|---|---|---|
| | Ba (mol.%) | Sr (mol.%) | Co (mol.%) | Fe (mol.%) | Ba/Sr (mole ratio) | Co/Fe (mole ratio) | A site/B site (mole ratio) |
| pH5-BSCF | 39.45 | 26.03 | 27.78 | 6.74 | 0.97 | 3.91 | 0.99 |
| pH6-BSCF | 39.58 | 26.08 | 27.68 | 6.66 | 0.97 | 3.94 | 0.99 |
| pH8-BSCF | 38.13 | 26.62 | 28.42 | 6.82 | 0.91 | 3.95 | 0.96 |
| pH9-BSCF | 37.27 | 26.86 | 28.91 | 6.96 | 0.89 | 3.94 | 0.94 |
| pH10-BSCF | 39.19 | 26.13 | 27.90 | 6.78 | 0.96 | 3.90 | 0.98 |

| | EDS | | | |
|---|---|---|---|---|
| | Ba (mol.%) | Sr (mol.%) | Co (mol.%) | Fe (mol.%) |
| pH5-BSCF | 25.74 ± 1.41 | 27.09 ± 0.54 | 37.42 ± 1.80 | 9.750 ± 0.69 |
| pH6-BSCF | 23.92 ± 0.30 | 26.79 ± 0.74 | 39.00 ± 0.57 | 10.29 ± 0.21 |
| pH8-BSCF | 22.92 ± 0.35 | 26.36 ± 0.62 | 40.12 ± 0.40 | 10.60 ± 0.22 |
| pH9-BSCF | 21.83 ± 0.45 | 28.24 ± 1.37 | 40.13 ± 0.79 | 9.800 ± 0.36 |
| pH10-BSCF | 23.42 ± 0.30 | 27.55 ± 0.47 | 39.09 ± 0.55 | 9.940 ± 0.21 |

0.11 Ω $cm^2$, respectively, at an operating temperature of 800 °C. Figure 8 shows the $R_2$ and $R_3$ polarization resistance versus temperature relationship, and Table 4 shows the calculated activation energy. The activation energies of $R_2$ were 125, 74, 113, 102, and 100 kJ/mole for the pH5-BSCF, pH6-BSCF, pH8-BSCF, pH9-BSCF, and pH10-BSCF samples, respectively. The activation energies of $R_3$ were 126, 136, 88, 97, and 51 kJ/mole for the pH5-BSCF, pH6-BSCF, pH8-BSCF, pH9-BSCF, and pH10-BSCF samples, respectively. These values are lower than those of LSCF, which was to be 135–142 kJ/mole [21]. Shao et al. [6] reported that the activation energy of polarization resistance of BSCF was 116 kJ/mol in the temperature range from 400 to 725 °C. In this study, the pH6-BSCF sample exhibited the lowest ASR and activation energy of charge transfer resistance due to the higher electronic conductivity of BSCF6 sample. The pH6-BSCF sample had higher activation energy of oxygen diffusion resistance comparing to the other samples, such as pH9-BSCF and pH10-BSCF. This is typical value for the stoichiometric BSCF oxygen conductor [20]. Since oxygen reduction occurs both on triple-phase-boundary (TPB) and the surface of a mixed ionic and electronic conductor (MIEC), BSCF is more active than that of the conventional pure electronic cathode electrode, such as $La_{0.8}Sr_{0.2}MnO_3$, where oxygen reduction occurs only on the TPB area. Therefore, the oxygen diffusion of an MIEC electrode strongly depends on the composition stoichiometry and elements distribution variation.

Table 5 shows the ICP-MS and EDS analysis of the BSCF powders, confirming the composition of the materials. All element content from the EDS analysis based on a standard $Ba_{0.5}Sr_{0.5}Co_{0.8}Fe_{0.2}O_{3-\delta}$ sample which was prepared by solid state reaction and the content was identified by ICP-MS. It is well known that EDS is not a particularly accurate method to determine atomic concentrations. ICP-MS is a more accurate technique to determine atomic concentrations. Therefore, the atomic concentrations of all elements were determined from ICP-MS method not from the EDS in this manuscript. However, the data of ICP-MS cannot show the composition distribution of samples [22]; therefore, we show the composition variation of samples by EDS analysis even the accuracy can be compared to ICP-MS. The ICP-MS results show that the BSCF6 sample prepared from the precursor solution with a pH value of 6 had the best stoichiometric ratio. Future, EDS results show that the element distribution is more homogeneous compared to the other samples, especially for Ba, Co, and Fe elements. This is the major reason why BSCF6 exhibits better conductivity and electrochemical performance than the other samples. These results suggest that the pH value of the precursor solution affects the chelating between the EDTA or citric acid and metal cations. Therefore, the composition of BSCF samples is different after heat treatment and affects the performance of BSCF electrodes.

## Conclusion

Perovskite oxide BSCF oxides were successfully synthesized by the citric–edta complexing method from precursor solutions with different pH values. All the samples exhibited similar crystals, lattice parameters, porosity, and microstructures. However, the chemical composition and element homogeneity of the samples were different, leading to different levels of conductivity and electrochemical performance. The BSCF powder prepared from the precursor solution with a pH value of 6 has the best stoichiometric ratio of composition and exhibits the highest conductivity of 50.2 S/cm at 400 °C, which is 1.3 times higher than the sample prepared from the precursor solution with a pH value of 9. The polarization resistance values for charge transfer and oxygen diffusion are 0.07 and 0.11 Ω $cm^2$ at 800 °C, respectively.

**Acknowledgements** This study was supported by the National Science Council of Taiwan (NSC 96-2221-E-155-053 and NSC 97-2221-E-155-059).

## References

1. Minh NQ (1993) J Am Ceram Soc 76:563
2. Adler SB, Lane JA, Steele BCH (1996) J Electrochem Soc 143:3554
3. Teraoka Y, Zhang HM, Furukawa S, Yamazoe N (1985) Chem Lett 167:1743
4. Huang K, Wan J, Goodenough JB (2001) J Mater Sci 36:1093. doi:10.1023/A:1004813305237
5. Shao ZP, Yang WS, Cong Y, Dong H, Tong J, Xiong GX (2000) J Membr Sci 172:177
6. Shao ZP, Haile SM (2004) Nature 431:170
7. Uchida H, Yoshida M, Watanabe M (1999) J Electrochem Soc 146:1
8. Kharton VV, Naumovich EN, Kovalevsky AV, Viskup AP, Figueiredo FM, Bashmakov IA, Marques FMB (2000) Solid State Ion 138:135
9. Tan L, Gu X, Yang L, Jin W, Zhang L, Xu N (2003) J Membr Sci 212:157
10. Wei B, Lu Z, Huang X, Miao J, Sha X, Xin X, Su W (2006) J Euro Ceram Soc 26:2827
11. Mosadeghkhah A, Alaee MA, Mohammadi T (2007) Mater Des 28:1699
12. Lee S, Lim Y, Lee EA, Hwang HJ, Moon JW (2006) J Power Sourc 157:848
13. Carter S, Selcuk A, Chater RJ, Kajda J, Kilner JA, Steele BCH (1992) Solid State Ion 53–56:597
14. Li S, Lu Z, Wei B, Huang X, Miao J, Cao G, Zhu R, Su W (2006) J Alloy Compd 426:408
15. Chen Z, Ran R, Zhou W, Shao Z, Liu S (2007) Electrochim Acta 52:7343
16. Tai LW, Nasrallah MM, Anerson HU, Sparlin DM, Sehlin SR (1995) Solid State Ion 76:259

17. Shao ZP, Haile SM, Ahn J, Ronney PD, Zhan ZL, Barnett SA (2005) Nature 435:795
18. Wang Y, Wang S, Wang Z, Wen T, Wen Z (2007) J Alloy Compd 428:286
19. Li S, Zhe L, Ai N, Chen K, Su W (2007) J Power Sourc 165:97
20. Baumann FS, Fleig J, Habermeier HU, Maier J (2006) Solid State Ion 177:3187
21. Hwang HJ, Moon JW, Lee S, Lee EA (2005) J Power Sourc 145:243
22. Yang CCT, Cho HJ, Wei WJ (2002) J Eur Ceram Soc 22:199